

# Ethylenedioxy-Containing Tetrathiapentalene Derivative with Ethylthio Chains, C<sub>2</sub>TEO-TTP

Shinya Kimura, Hirofumi Nii, Hiroyuki Kurai, Tomoaki Takeuchi, Mao Katsuhara, and Takehiko Mori\*

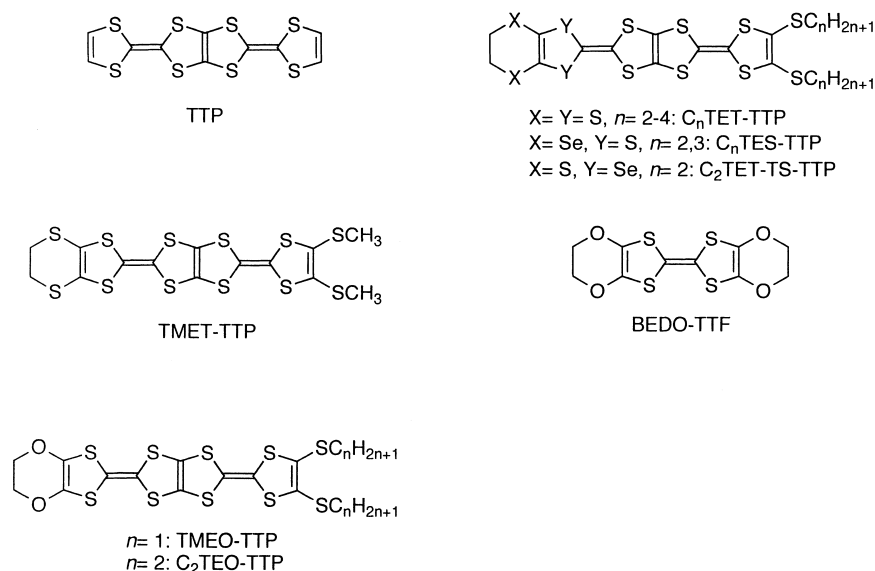
Department of Organic and Polymeric Materials, Tokyo Institute of Technology, O-okayama, Tokyo 152-8552

(Received May 7, 2002)

A new oxygen-containing  $\pi$ -electron donor having ethylthio chains, C<sub>2</sub>TEO-TTP (2-[4,5-bis(ethylthio)-1,3-dithiol-2-ylidene]-5-(4,5-ethylenedithio-1,3-dithiol-2-ylidene)-1,3,4,6-tetrathiapentalene), has been synthesized. Single-component C<sub>2</sub>TEO-TTP forms a  $\beta'$ -like dimerized structure. The 2:1 salts with PF<sub>6</sub><sup>−</sup>, ClO<sub>4</sub><sup>−</sup>, and AsF<sub>6</sub><sup>−</sup> have a uniform  $\beta$ -type structure isostructural to the ethylenedithio analog, (C<sub>2</sub>TET-TTP)<sub>2</sub>ClO<sub>4</sub>, and are metallic down to liquid helium temperatures. On the other hand, (C<sub>2</sub>TEO-TTP)<sub>2</sub>Au(CN)<sub>2</sub> has dimeric donor arrangement, and shows hysteretic temperature dependence of the conductivity.

Recently, tetrathiapentalene<sup>1</sup> (TTP, Scheme 1) derivatives having alkylthio chains: C<sub>n</sub>TET-TTP ( $n = 2$ –4, Scheme 1),<sup>2</sup> C<sub>n</sub>TES-TTP ( $n = 2, 3$ , Scheme 1),<sup>3</sup> and C<sub>2</sub>TET-TS-TTP (Scheme 1),<sup>4</sup> have been prepared. Investigation of these donors demonstrates that the replacement of the methylthio chains with ethylthio chains is a promising modification of TTP derivatives, especially for modifications derived from TMET-TTP (Scheme 1).<sup>5</sup> Changing the alkyl length, one can control not only the anion contents but also the donor arrangements. In particular, the C<sub>2</sub> salts prefer a uniform  $\beta$ -structure;<sup>6</sup> the same structure has been found in many radical-cation salts such as (C<sub>2</sub>TET-TTP)<sub>2</sub>ClO<sub>4</sub> and (C<sub>2</sub>TET-TS-TTP)<sub>2</sub>X (X = BF<sub>4</sub>, ClO<sub>4</sub>, and PF<sub>6</sub>). These salts exhibit metallic conductivity down to low temperatures. On the other hand, many metallic

conductors of BEDO-TTF (Scheme 1) have been prepared, where attachment of the ethylenedioxy groups constructs a CH $\cdots$ O network.<sup>7</sup> The ethylenedioxy moiety has strong tendency to result in ring-over-atom overlap, so that most of BEDO-TTF salts have the  $\beta''$ -structure. Even in TTP donors, introduction of the ethylenedioxy part gives rise to a  $\beta''$ -structure; (TMEO-TTP)<sub>2</sub>Au(CN)<sub>2</sub> (Scheme 1) is the only  $\beta''$ -structure found in TTP salts.<sup>8</sup> From this viewpoint, it is interesting to learn whether introduction of an ethylenedioxy part to C<sub>2</sub>TET-TTP (namely C<sub>2</sub>TEO-TTP, Scheme 1) will destroy the uniform  $\beta$ -structure or not. This donor is regarded as an extension of the methylthio chains of TMET-TTP to ethylthio chains. In this paper, synthesis, structures, and physical properties of the charge-transfer salts of C<sub>2</sub>TEO-TTP are described.



Scheme 1.

## Experimental

**Synthesis.** Synthesis of C<sub>2</sub>TEO-TTP was achieved as shown in Scheme 2. In the previous report, 5-(4,5-ethylenedioxy-1,3-dithiol-2-ylidene)-1,3,4,6-tetrathiapentalen-2-one (**5**) was synthesized by deprotection of benzoyl groups followed by the treatment with triphosgene (bis(trichloromethyl) carbonate).<sup>9</sup> In this work, however, the method via 2,3-bis(2-cyanoethylthio)-6,7-ethylenedioxytetrathiafulvalene (**4**) was used, due to the improved yield and the more simple synthetic operation.<sup>10</sup>

Compound **4** was obtained by triethyl phosphite-mediated cross coupling between **2**<sup>11</sup> and **3**<sup>12</sup> in 23% yield. The cyanoethyl groups of **4** were removed by cesium hydroxide, and the following treatment with triphosgene provided **5** in 62% yield. Compounds **5** and 4,5-bis(ethylthio)-1,3-dithiole-2-thione (**6**)<sup>13</sup> were cross-coupled in trimethyl phosphite to give C<sub>2</sub>TEO-TTP (**1**) in 17.4% yield.

**General Data.** Trimethyl phosphite and triethyl phosphite were distilled under nitrogen by fractional distillation. Methanol was distilled under nitrogen over magnesium methoxide. Acetone was used after the storage over Molecular Sieves 4A. THF was freshly distilled under nitrogen over sodium and benzophenone. Melting points were determined with a Yanaco MP micro melting point apparatus. NMR spectra were obtained with a JEOL JNM-AL300 spectrometer and cyclic voltammetry data were measured by a Yanaco VMA-010 recorder. IR spectra were recorded on a SHIMADZU FTIR-8000 spectrometer, and mass spectra on a SHIMADZU QP-5000 spectrometer. Microanalyses were performed at Microanalytical Laboratory, Tokyo Institute of Technology. In the microanalyses, errors of  $\pm 1.5\%$  should be allowed for the S values of the compounds containing over 50% sulfur.

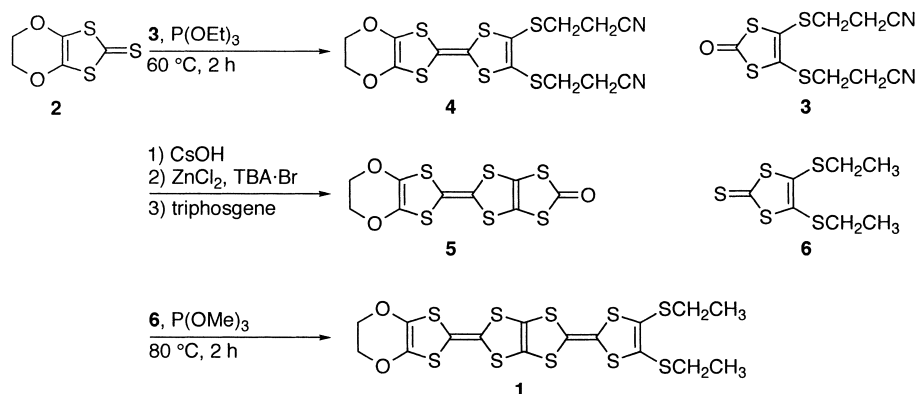
**2,3-Bis(2-cyanoethylthio)-6,7-ethylenedioxytetrathiafulvalene (4).** Compounds **2** (1.74 g, 9.1 mmol) and **3** (2.61 g, 9.1 mmol) were heated at 80 °C in triethyl phosphite (65 mL) under argon for 1 h. After the mixture was cooled to room temperature, the solvent was removed in vacuo. The residue was purified by column chromatography (silica gel, CH<sub>2</sub>Cl<sub>2</sub>–hexane) to afford **4** (980 mg, 23%) as an orange solid. mp 135–136 °C (dec.); IR (KBr) 2985 (s), 2951 (m), 2921 (m), 2250 (m), 1770 (w), 1667 (s), 1614 (s), 1481 (w), 1421 (s), 1326 (w), 1281 (s), 1158 (s), 959 (w), 886 (s), 738 (m), 725 (w), 463 (w) cm<sup>-1</sup>; <sup>1</sup>H NMR (CDCl<sub>3</sub>)  $\delta$  1.31 (4H, t,  $J = 7.0$  Hz), 2.82 (4H, t,  $J = 7.0$  Hz), 4.23 (4H, s); Anal. Calcd for C<sub>14</sub>H<sub>12</sub>N<sub>2</sub>O<sub>2</sub>S<sub>6</sub>: C, 38.87; H, 2.80; N, 6.48; O, 7.40; S, 44.46%. Found: C, 38.88; H, 2.66; N, 6.49; O, 7.80; S, 44.21%.

**5-(4,5-Ethylenedioxy-1,3-dithiol-2-ylidene)-1,3,4,6-tetrathiapentalen-2-one (5).** To a mixture of **4** (0.72 g, 1.7 mmol) and cesium hydroxide (2.1 g, 14 mmol) were added acetone (12 mL) and methanol (12 mL) at 0 °C under argon, and the reaction mixture was then stirred for 30 min at room temperature. The mixture was treated at 0 °C with anhydrous zinc chloride (0.12 mg, 0.85 mmol) dissolved in methanol (4.5 mL) and with tetrabutylammonium bromide (0.54 mg, 1.7 mmol) dissolved in methanol (4.5 mL). After stirring at room temperature for 15 min, the reaction mixture was filtered. The residue was suspended in THF (18 mL) and an excess of triphosgene (1.01 g, 3.4 mmol) dissolved in THF (6 mL) was added at –78 °C. The reaction mixture was allowed to warm up to room temperature overnight and filtered. The residue was purified by short column chromatography (silica gel, CS<sub>2</sub>) to afford **5** (370 mg, 62%) as a gold solid. mp 200 °C (dec.); IR (KBr) 2924 (w), 1680 (s), 1651 (m), 1459 (w), 1268 (w), 1194 (w), 1167 (s), 1084 (w), 1013 (w), 949 (w), 861 (w) cm<sup>-1</sup>; <sup>1</sup>H NMR (CDCl<sub>3</sub>)  $\delta$  4.27 (4H, s); Anal. Calcd for C<sub>9</sub>H<sub>4</sub>O<sub>3</sub>S<sub>6</sub>·0.2THF: C, 32.33; H, 1.55; S, 52.85%. Found: C, 32.34; H, 1.65; S, 54.12%.

**C<sub>2</sub>TEO-TTP (1).** Compound **5** (397 mg, 1.12 mmol) and **6** (714 mg, 2.76 mmol) were heated at 90 °C in trimethyl phosphite (17 mL) for 2 h. After the mixture was cooled to room temperature, the solvent was removed in vacuo and purified by column chromatography (silica gel, CS<sub>2</sub>) to afford **1** (110 mg, 17%) as a red solid. mp 188–189 °C (dec.); IR (KBr) 2920 (w), 1656 (w), 1262 (w), 1164 (w), 1084 (w), 1010 (w), 950 (w), 881 (w), 862 (w), 761 (w) cm<sup>-1</sup>; <sup>1</sup>H NMR (CDCl<sub>3</sub>)  $\delta$  1.31 (6H, t,  $J = 7.4$  Hz), 2.82 (4H, q,  $J = 7.4$  Hz), 4.23 (4H, s); Anal. Calcd for C<sub>16</sub>H<sub>14</sub>O<sub>2</sub>S<sub>10</sub>: C, 34.39; H, 2.52; S, 57.36%. Found: C, 34.49; H, 2.49; S, 56.76%.

**Cyclic Voltammetry.** The electrochemical properties of newly synthesized donor, C<sub>2</sub>TEO-TTP, were investigated by cyclic voltammetry in benzonitrile in the presence of *n*-Bu<sub>4</sub>NPF<sub>6</sub> as a supporting electrolyte ( $1.3 \times 10^{-2}$  mol L<sup>-1</sup>) using Pt working and counter electrodes and an Ag<sup>+</sup>/AgCl reference electrode at 25 °C.

**X-ray Diffractational Analysis.** The data were collected on a Rigaku AFC7R diffractometer with graphite monochromated Mo K $\alpha$  radiation and a rotating anode generator using the  $2\theta$ – $\omega$  and  $\omega$  scan techniques to a maximum  $2\theta$  of 60°. The structure was solved by the direct method and refined by full-matrix least-squares analysis (anisotropic for non-hydrogen atoms). Unit weight was used for the least-squares refinement of the PF<sub>6</sub> and ClO<sub>4</sub> salts, because the weighting scheme based on counting statistics did not converge. All calculations were performed using

Scheme 2. Synthesis of C<sub>2</sub>TEO-TTP.

the teXsan crystallographic software package of Molecular Structure Corporation.

Crystallographic data have been deposited at the CCDC, 12 Union Road, Cambridge CB2 1EZ, UK and copies can be obtained on request, free of charge, by quoting the publication citation and the deposition numbers 184986–184990.

## Results and Discussion

**Electrochemical Properties.** The donor displayed four pairs of redox waves corresponding to one-electron transfer processes. The redox potentials are summarized in Table 1. The comparison of the values with C<sub>2</sub>TET-TTP reveals that the first oxidation potential  $E_1$  as well as the  $E_2 - E_1$  value, which is a measure of the on-site Coulomb repulsion, are nearly the same. This suggests that the replacement of an ethylenedithio group of C<sub>2</sub>TET-TTP with an ethylenedioxy group does not much change the electron-donating ability.

**X-ray Analysis of Single-Component Crystal.** By slow evaporation of the dichloromethane-methanol solution, single-component crystals of C<sub>2</sub>TEO-TTP were obtained as red needle-shaped crystals, with sufficient quality for X-ray analysis. The crystal data are summarized in Table 2.

The molecular structure is shown in Fig. 1. As shown in Fig. 1(b), the TTP moiety including the ethylenedioxy ring is almost flat, and the two ethylthio chains extend out of the molecular plane with a tilt to the inner direction. Figure 2 shows the crystal structure of C<sub>2</sub>TEO-TTP. In this structure, one crystallographically independent donor is located on a general position, constructing a dimeric structure. The donor arrangement projected along the molecular long axis (Fig. 2(b)) is  $\beta'$ -

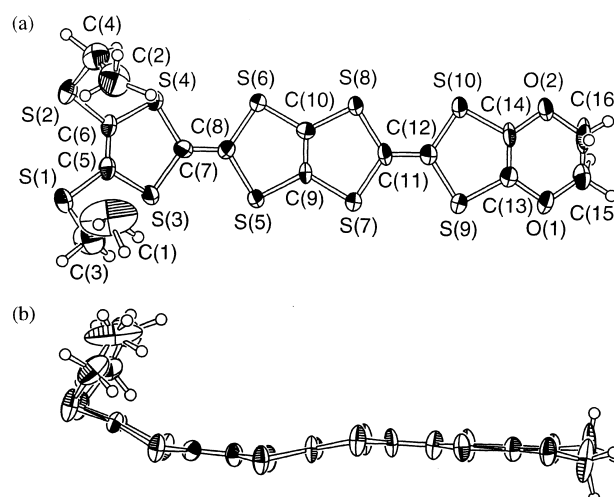


Fig. 1. (a) ORTEP drawing and atomic numbering scheme and (b) side view of the donor molecule of C<sub>2</sub>TEO-TTP.

Table 1. Redox Potentials of C<sub>2</sub>TEO-TTP Compared with C<sub>2</sub>TET-TTP(V)

Compound	$E_1$	$E_2$	$E_3$	$E_4$	$E_2 - E_1$
C <sub>2</sub> TEO-TTP	+0.46	+0.70	+0.94	+1.08	0.24
C <sub>2</sub> TET-TTP	+0.44	+0.68	+0.94	+1.18	0.24

vs Ag/AgCl in Bu<sub>4</sub>NPF<sub>6</sub>/PhCN.

Table 2. Crystallographic Data of C<sub>2</sub>TEO-TTP.

Chemical formula	C <sub>16</sub> H <sub>14</sub> O <sub>2</sub> S <sub>10</sub>		
Formula weight	558.89		
Shape	red needle		
Crystal system	triclinic		
Space group	<i>P</i> $\bar{1}$		
<i>a</i> /Å	12.435(6)	$\alpha$ /°	93.32(4)
<i>b</i> /Å	12.457(5)	$\beta$ /°	104.85(4)
<i>c</i> /Å	7.639(3)	$\gamma$ /°	83.52(4)
<i>V</i> /Å <sup>3</sup>	1136.0(9)		
<i>Z</i>	2		
<i>D</i> <sub>calc</sub> /g cm <sup>−3</sup>	1.634		
$\lambda$ /Å	0.71070		
<i>T</i> /K	298		
Weighting scheme <sup>a)</sup>	$w = [\sigma_c^2(F_o) + (0.0162)^2 F_o^2/4]^{-1}$		
<i>R</i> <sup>b)</sup>	0.051	<i>R</i> <sub>w</sub> <sup>c)</sup>	0.073
Reflections used	1759 ( <i>I</i> > 3.0 $\sigma(I)$ )		

a)  $\sigma_c(F_o)$  = e.s.d based on counting statistics. b)  $R = \sum ||F_o| - |F_c|| / \sum |F_o|$ . c)  $R_w = [\sum w(|F_o| - |F_c|)^2 / \sum w F_o^2]^{1/2}$ .

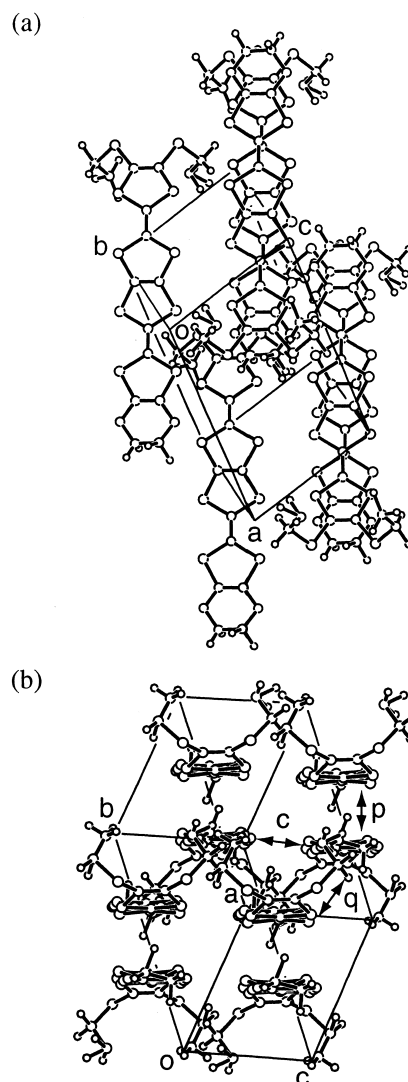


Fig. 2. Crystal structure of C<sub>2</sub>TEO-TTP, (a) projected in the stacking direction and (b) projected along the molecular long axis. The overlap integrals are  $p = 6.9$ ,  $q = 2.4$ , and  $c = -6.6 \times 10^{-3}$ .

type.<sup>6</sup> Overlap integrals of HOMO (Fig. 2(b)) are  $p = 6.9$ ,  $q = 2.4$ , and  $c = -6.6 \times 10^{-3}$ . The overlap mode in the dimer is the so-called ring-over-bond type; the interplane distance is 3.69 Å and the slip distance along the donor long axis is 1.11 Å.

**Preparation and Electrical Properties of Charge-Transfer Complexes.** This donor, C<sub>2</sub>TEO-TTP, is as soluble in organic solvents as C<sub>2</sub>TET-TTP. All charge-transfer complexes were prepared by electrochemical oxidation in chlorobenzene at 25–28 °C in the presence of tetrabutylammonium salts of various anions. The obtained salts are summarized in Table 3. The temperature-dependent resistivity is shown in Fig. 3. This donor, C<sub>2</sub>TEO-TTP (**1**) forms complexes with PF<sub>6</sub><sup>−</sup>, ClO<sub>4</sub><sup>−</sup>, AsF<sub>6</sub><sup>−</sup>, and Au(CN)<sub>2</sub><sup>−</sup> in the form of black needles. The compositions are found to be 2:1 by X-ray structure analyses. Among them, the PF<sub>6</sub>, ClO<sub>4</sub>, and AsF<sub>6</sub> salts exhibit high electrical conductivities at room temperature: 380, 560, and 500 S cm<sup>−1</sup>, respectively. These salts show metallic conductivity down to helium temperatures.

On the other hand, (C<sub>2</sub>TEO-TTP)<sub>2</sub>Au(CN)<sub>2</sub> shows quite different conducting behavior. The room-temperature conductivity is 11 S cm<sup>−1</sup>. As temperature lowers, the resistivity gradually decreases with several jumps. During the heating process, the resistivity gradually increases as temperature rises, and then suddenly drops around 250 K. This type of hysteretic temperature dependence is similar to (TMEO-TTP)<sub>2</sub>Au(CN)<sub>2</sub>.<sup>8</sup>

**Crystal and Electronic Structures of the C<sub>2</sub>TEO-TTP Salts.** X-ray single crystal structure analyses and band calculations were carried out for (C<sub>2</sub>TEO-TTP)<sub>2</sub>X (X = PF<sub>6</sub>, ClO<sub>4</sub>, AsF<sub>6</sub>, and Au(CN)<sub>2</sub>). Although the *R* factors of the PF<sub>6</sub> and

ClO<sub>4</sub> salts are large owing to the poor crystal quality, the results are sufficient for the following qualitative discussion.

The lattice parameters in Table 4 indicate that the PF<sub>6</sub>, ClO<sub>4</sub>, and AsF<sub>6</sub> salts are isostructural to (C<sub>2</sub>TET-TTP)<sub>2</sub>ClO<sub>4</sub>. The donor molecular structure of (C<sub>2</sub>TEO-TTP)<sub>2</sub>AsF<sub>6</sub> is shown in Fig. 4. As shown in Fig. 4(b), the almost flat TTP moiety and the conformation of the ethylenedichalcogeno ring are the same as those of (C<sub>2</sub>TET-TTP)<sub>2</sub>ClO<sub>4</sub>. Figure 5 shows the crystal structure of (C<sub>2</sub>TEO-TTP)<sub>2</sub>AsF<sub>6</sub>. The shapes of AsF<sub>6</sub><sup>−</sup> and ClO<sub>4</sub><sup>−</sup> are not the same, but the As and Cl atoms locate on the same general position. In the series of the C<sub>2</sub>TEO-TTP salts, the donors are stacked in a head-to-head manner (Fig. 6). The overlap modes are the so-called ring-over-bond type: the interplane distances are 3.45 Å for the PF<sub>6</sub> salt, 3.44 Å for the ClO<sub>4</sub> salt, and 3.47 Å for the AsF<sub>6</sub> salt. The slips along the molecular long axis are 4.55 Å, 4.53 Å, and 4.55 Å, respectively. Donor arrangement of (C<sub>2</sub>TEO-TTP)<sub>2</sub>AsF<sub>6</sub> is shown in Fig. 7, and the arrows drawn between the donor molecules indicate the overlap integrals:  $b = -16.4$ ,  $p_1 = 2.5$ ,  $p_2 = 5.7$ ,  $p_3 = 1.2$ , and  $p_4 = 8.5 \times 10^{-3}$ . Similar values are found for the other two salts:  $b = -17.0$ ,  $p_1 = 2.4$ ,  $p_2 = 5.9$ ,  $p_3 = 1.2$ , and  $p_4 = 8.7 \times 10^{-3}$  for the PF<sub>6</sub> salt, and  $b = -15.7$ ,  $p_1 = 2.5$ ,  $p_2 = 7.3$ ,  $p_3 = 0.9$ , and  $p_4 = 9.1 \times 10^{-3}$  for the ClO<sub>4</sub> salt. To discuss the effect of the chalcogen exchange, it is important to compare the intrachain overlap (the *b* interaction) and the largest interchain overlap (the *p*<sub>4</sub> interaction). As shown in Ref. 2, the value of  $|p_4/b|$ , representing the magnitude of the side-by-

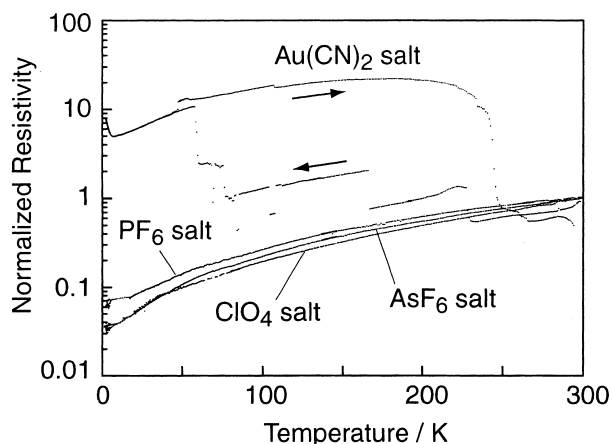


Fig. 3. Temperature dependence of the resistivities of C<sub>2</sub>TEO-TTP salts (normalized to the values at room temperature).

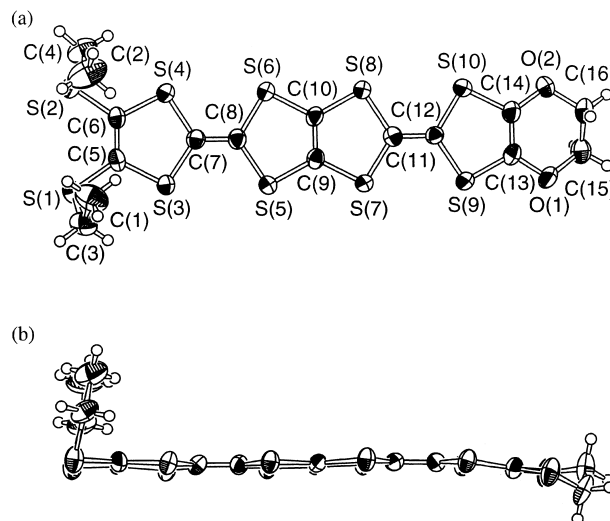


Fig. 4. (a) ORTEP drawing and atomic numbering scheme and (b) side view of the donor molecule in (C<sub>2</sub>TEO-TTP)<sub>2</sub>AsF<sub>6</sub>.

Table 3. Composition and Conductivity of Charge-Transfer Complexes of (C<sub>2</sub>TEO-TTP)<sub>2</sub>A<sub>x</sub>

Anion (A)	Form	<i>x</i> <sup>a)</sup>	$\sigma_{\text{rt}}/\text{S cm}^{-1}$	Conducting behavior
PF <sub>6</sub>	black needle	0.5	380	M down to 0.5 K <sup>b)</sup>
ClO <sub>4</sub>	black needle	0.5	560	M down to 0.5 K <sup>b)</sup>
AsF <sub>6</sub>	black needle	0.5	500	M down to 0.5 K <sup>b)</sup>
Au(CN) <sub>2</sub>	black needle	0.5	11	Hysteretic <sup>c)</sup>

a) Determined from the X-ray single crystal analysis. b) M = Metallic. c) M–M transition was observed with hysteresis.

Table 4. Crystallographic Data of  $(C_2TEO-TTP)_2X$  ( $X = PF_6$ ,  $ClO_4$ , and  $AsF_6$ )

X	$PF_6$	$ClO_4$	$AsF_6$
Chemical formula	$C_{32}H_{28}F_6O_4PS_{20}$	$C_{32}H_{28}ClO_8S_{20}$	$C_{32}H_{28}AsF_6O_4S_{20}$
Formula weight	1262.73	1217.22	1306.68
Shape	black needle	black needle	black needle
Crystal system	monoclinic	monoclinic	monoclinic
Space group	$C2/c$	$C2/c$	$C2/c$
$a/\text{\AA}$	24.63(1)	24.60(6)	24.656(1)
$b/\text{\AA}$	5.715(5)	5.700(4)	5.73(8)
$c/\text{\AA}$	34.50(2)	33.91(5)	34.87(6)
$\alpha/^\circ$	90	90	90
$\beta/^\circ$	102.93(4)	101.7(2)	103(2)
$\gamma/^\circ$	90	90	90
$V/\text{\AA}^3$	4732(4)	4655(13)	4792(52)
Z	4	4	4
$D_{\text{calc}}/\text{g cm}^{-3}$	1.772	1.737	1.811
$\lambda/\text{\AA}$	0.71069	0.71069	0.71069
T/K	298	298	298
Weighting scheme <sup>a)</sup>	unit weight	unit weight	$w = 1/\sigma_c^2(F_o)$
$R^b$	0.157	0.170	0.048
$R_w^c$	0.194	0.188	0.026
Reflections used	1445 ( $I > 3.0 \sigma(I)$ )	2338 ( $I > 5.0 \sigma(I)$ )	1821 ( $I > 3.0 \sigma(I)$ )

a)  $\sigma_c(F_o) = \text{e.s.d based on counting statistics}$ . b)  $R = \Sigma ||F_o| - |F_c|| / \Sigma |F_o|$ . c)  $R_w = [\Sigma w(|F_o| - |F_c|)^2 / \Sigma w F_o^2]^{1/2}$ .

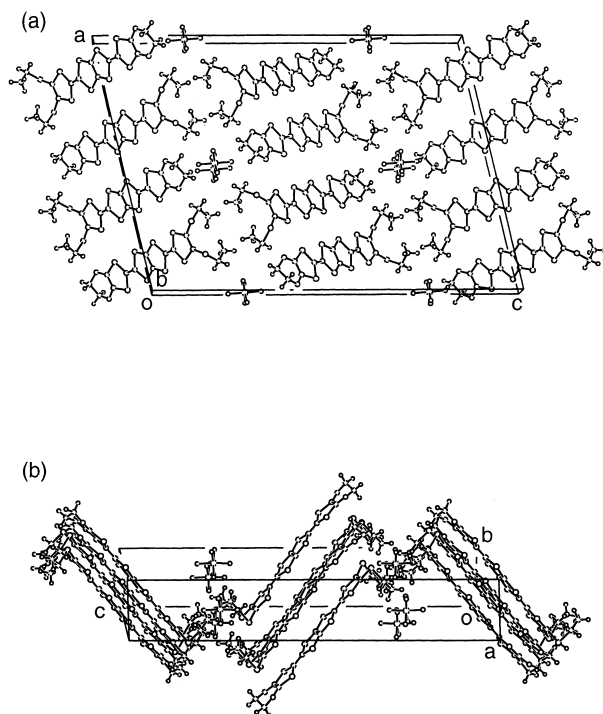


Fig. 5. Crystal structure of  $(C_2TEO-TTP)_2AsF_6$ , (a) projected along the  $b$  axis and (b) projected along the molecular short axis.

side interaction, is 0.58 for  $(C_2TEO-TTP)_2ClO_4$  in comparison with 0.48 for  $(C_2TET-TTP)_2ClO_4$ , indicating that replacement of an ethylenedithio ring of  $C_2TET-TTP$  with an ethylenedioxy ring increases the two-dimensionality. Figure 8 shows the energy band structures and Fermi surfaces. Although the energy

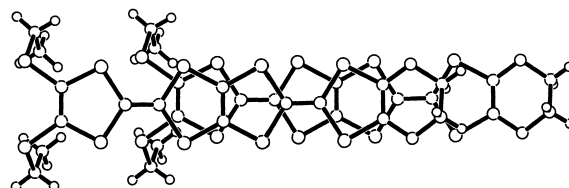


Fig. 6. Overlap mode of  $(C_2TEO-TTP)_2AsF_6$ .

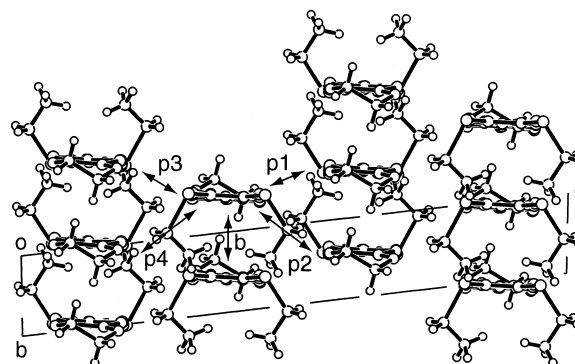


Fig. 7. Donor arrangement of  $(C_2TEO-TTP)_2AsF_6$ . The overlap integrals are  $b = -16.4$ ,  $p1 = 2.5$ ,  $p2 = 5.7$ ,  $p3 = 1.2$ , and  $p4 = 8.5 \times 10^{-3}$ .

band of  $(C_2TEO-TTP)_2ClO_4$  has a very small gap on the  $k_a$  axis accidentally, the energy bands and Fermi surfaces of these three compounds are basically the same.

On the other hand, the  $Au(CN)_2$  salt has a quite different structure. The crystal data are summarized in Table 5. The donor molecular structure of  $(C_2TEO-TTP)_2Au(CN)_2$  is shown in Fig. 9. Figure 9(b) shows that the TTP skeleton of the donor molecule is almost flat. Similarly to  $(C_2TEO-TTP)_2X$  ( $X =$

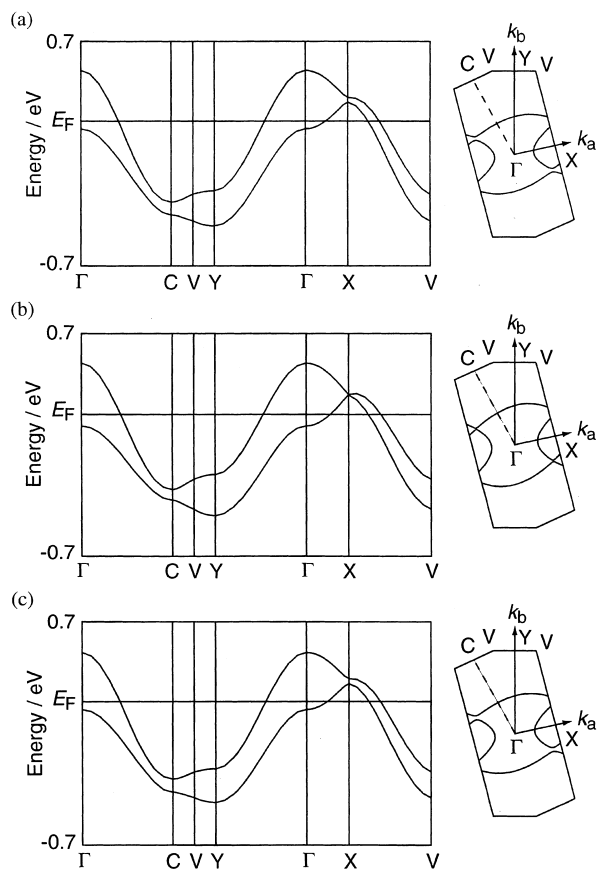


Fig. 8. Energy band structure and Fermi surface of  $(\text{C}_2\text{TEO-TTP})_2\text{X}$  ( $\text{X} =$  (a)  $\text{PF}_6$ , (b)  $\text{ClO}_4$ , and (c)  $\text{AsF}_6$ ).

Table 5. Crystallographic Data of  $(\text{C}_2\text{TEO-TTP})_2\text{Au}(\text{CN})_2$

Chemical formula	$\text{C}_{34}\text{H}_{28}\text{AuN}_2\text{O}_4\text{S}_{20}$		
Formula weight	1495.01		
Shape	black needle		
Space group	$P\bar{1}$		
$a/\text{\AA}$	8.215(4)	$\alpha/^\circ$	95.42(3)
$b/\text{\AA}$	20.387(7)	$\beta/^\circ$	105.15(4)
$c/\text{\AA}$	7.300(3)	$\gamma/^\circ$	91.85(4)
$V/\text{\AA}^3$	1173(1)		
$Z$	1		
$D_{\text{calc}}/\text{g cm}^{-3}$	2.117		
$\lambda/\text{\AA}$	0.71069		
$T/\text{K}$	298		
Weighting scheme <sup>a)</sup>	$w = [\sigma_c^2(F_o) + (0.0182)^2 F_o^2/4]^{-1}$		
$R^b$	0.062	$R_w^c$	0.059
Reflections used	1922 ( $I > 3.0 \sigma(I)$ )		

a)  $\sigma_c(F_o) = \text{e.s.d based on counting statistics}$ . b)  $R = \sum ||F_o| - |F_c|| / \sum |F_o|$ . c)  $R_w = [\sum w(|F_o| - |F_c|)^2 / \sum w F_o^2]^{1/2}$ .

$\text{PF}_6$ ,  $\text{ClO}_4$ , and  $\text{AsF}_6$ ), the ethylthio chains extend nearly perpendicular to the TTP skeleton, but the bending angle is smaller. Figures 10 and 11 show the crystal structure of  $(\text{C}_2\text{TEO-TTP})_2\text{Au}(\text{CN})_2$ . Different from the other  $\text{C}_2\text{TEO-TTP}$  salts, this salt has dimeric  $\beta$ -type structure.<sup>6</sup> Contrary to the 1:1 dimeric salts,  $(\text{C}_4\text{TET-TTP})\text{I}_3$  and  $(\text{C}_4\text{TES-TTP})\text{I}_3$ , this salt maintains segregated stacking. In this structure, one crystallo-

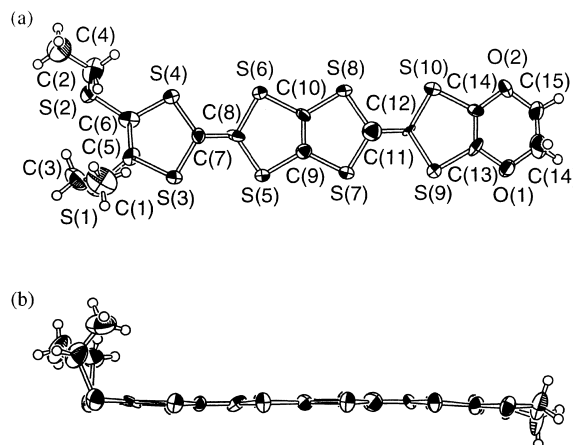


Fig. 9. (a) ORTEP drawing and atomic numbering scheme and (b) side view of the donor molecule of  $(\text{C}_2\text{TEO-TTP})_2\text{Au}(\text{CN})_2$ .

graphically independent donor molecule is located on a general position and one crystallographically independent anion molecule is on a special position of the inversion center, so the composition is 2:1. The origin of the dimeric structure is explained by the anion packing. Linear anions like  $\text{I}_3^-$  and  $\text{Au}(\text{CN})_2^-$  tend to align parallel to the donor stacking direction.<sup>8</sup> The lattice parameters along the stacking direction of the uniform-stacking salts,  $(\text{C}_2\text{TEO-TTP})_2\text{X}$  ( $\text{X} = \text{PF}_6$ ,  $\text{ClO}_4$ , and  $\text{AsF}_6$ ), are about 5.7 Å, which is too small for  $\text{Au}(\text{CN})_2^-$  (~7.7 Å, including the van der Waals radii). In consequence, the lattice parameter becomes twice as long, accompanied by the dimerization of the donors, so as to incorporate  $\text{Au}(\text{CN})_2^-$ . Figure 11 shows the two stacking manners of the donor molecules;  $p1$  and  $p2$  representing the intra- and interdimer overlaps. Both overlaps are so-called ring-over-bond types. The interplane distances are 3.43 Å for  $p1$  and 3.49 Å for  $p2$ . The slip distances along the donor long axis are 1.59 Å and 4.85 Å, respectively. As shown in Fig. 12, the calculated overlap integrals between the HOMOs are  $p1 = 26.8$ ,  $p2 = 16.6$ ,  $a = -2.0$ ,  $c1 = -2.6$ , and  $c3 = -7.3 \times 10^{-3}$ . The interdimer overlap (the  $p2$  interaction) is not so small compared with the intradimer overlap (the  $p1$  interaction). The interchain overlaps (the  $c1$ – $c3$  interactions) are moderately strong, resulting in a quasi-one-dimensional electronic structure. As shown in Fig. 13, the Fermi surface based on the tight-binding band structure calculated by using these overlap integrals is open, though the corrugation is significant. This is in accord with the quasi-one-dimensionality along the  $a+c$  columns.

## Conclusion

In order to introduce some instability in  $(\text{C}_2\text{TET-TTP})_2\text{-ClO}_4$ , which has very stable metallic conductivity down to low temperatures, selenium-containing analogs,  $\text{C}_2\text{TES-TTP}$  and  $\text{C}_2\text{TET-TS-TTP}$  have been synthesized. These donors have, however, formed only metallic complexes isostructural to  $(\text{C}_2\text{TET-TTP})_2\text{ClO}_4$ .<sup>2,4</sup> In the present  $\text{C}_2\text{TEO-TTP}$  donor, the introduction of the ethylenedioxy moiety is insufficient to bring about ring-over-atom ( $\beta''$ ) structure, but the isostructural uniform  $\beta$ -structure is realized in the tetrahedral and octahedral anions. Thus, as many as seven members with the  $\text{C}_2$

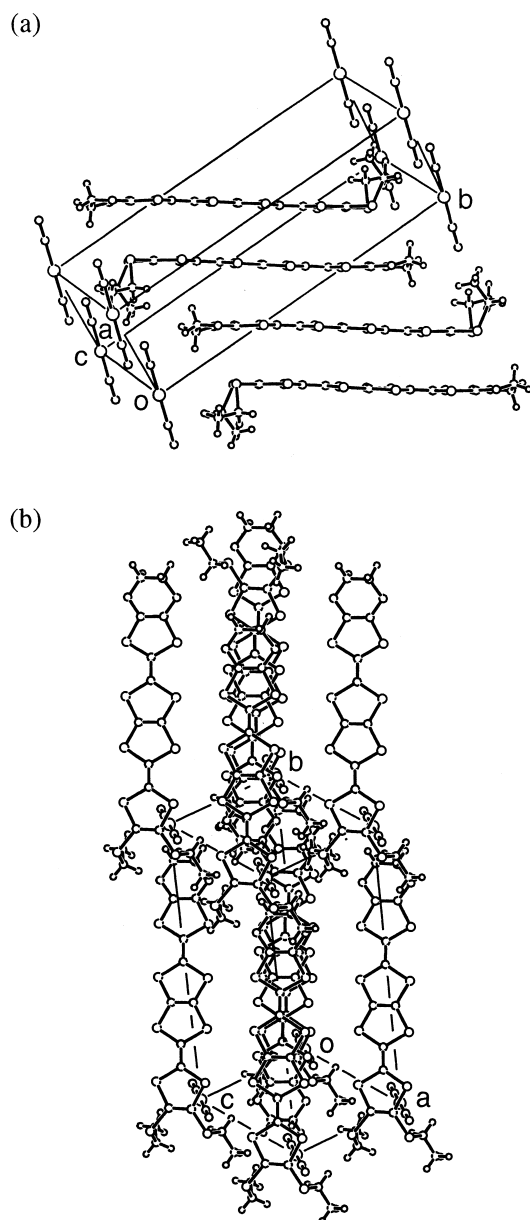


Fig. 10. Crystal structure of  $(\text{C}_2\text{TEO-TTP})_2\text{Au}(\text{CN})_2$ , (a) projected along the molecular short axis and (b) projected in the stacking direction.

chains, whose structures have been analyzed so far, fall into this isostructural series. This demonstrates the strong tendency of these  $\text{C}_2$  donors to form this uniform  $\beta$ -structure. The present  $(\text{C}_2\text{TEO-TTP})_2\text{Au}(\text{CN})_2$  salt affords a new structure, but the principle of the ring-over-bond stacking is the same, and the only difference is the introduction of dimerization owing to the long anions. Up to now, an attempt to prepare an  $\text{Au}(\text{CN})_2$  salt of  $\text{C}_2\text{TET-TTP}$  has not resulted in any crystals. Although control of donor arrangements by  $\text{CH}\cdots\text{O}$  interactions is not achieved, crystallizing ability is improved by the introduction of the ethylenedioxy ring. All  $\text{C}_2\text{TEO-TTP}$  salts obtained in this study have ring-over-bond type overlaps. This shows a remarkable contrast to the methylthio analog,  $\text{TMeO-TTP}$ , forming a  $\beta''$ -salt,  $(\text{TMeO-TTP})_2\text{Au}(\text{CN})_2$  with ring-over-atom type overlaps.<sup>8</sup>  $\text{TMET-TTP}$  also prefers ring-over-

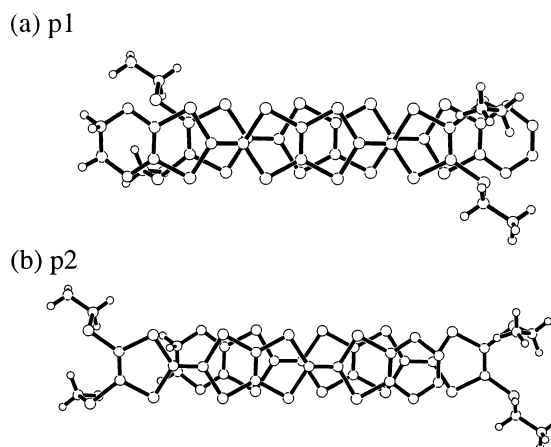


Fig. 11. (a) Intradimer and (b) interdimer overlap modes of  $(\text{C}_2\text{TEO-TTP})_2\text{Au}(\text{CN})_2$ .

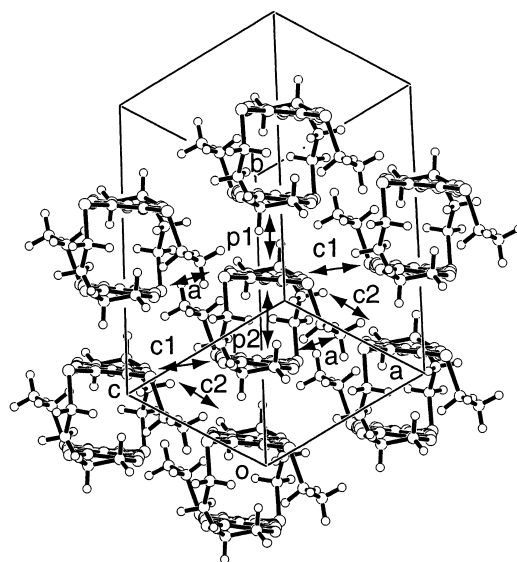


Fig. 12. Donor arrangement of  $(\text{C}_2\text{TEO-TTP})_2\text{Au}(\text{CN})_2$ . The overlap integrals are  $p1 = 26.8$ ,  $p2 = 16.6$ ,  $a = -2.0$ ,  $c1 = -2.6$ , and  $c2 = -7.3 \times 10^{-3}$ .

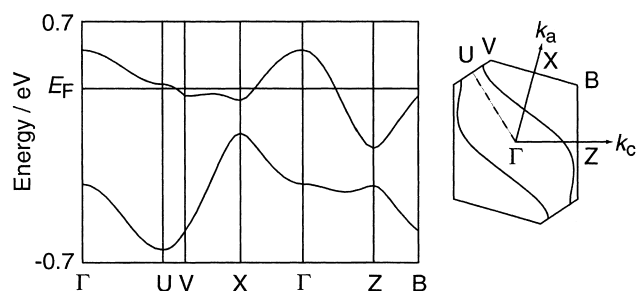


Fig. 13. Energy band structure and Fermi surface of  $(\text{C}_2\text{TEO-TTP})_2\text{Au}(\text{CN})_2$ .

atom overlap, because all  $\text{TMET-TTP}$  salts take  $\theta$ -type structures.<sup>14</sup> Thus there is a remarkable tendency: the  $\text{C}_1$  donor prefers the ring-over-atom overlap and the  $\text{C}_2$  donor forms the ring-over-bond overlap. This may be associated with the packing of the alkyl chains. The present work demonstrates that

this rule is superior to the preference of the ethylenedioxy (BEDO) part to the ring-over-atom overlap.

## References

- 1 Y. Misaki, H. Nishikawa, K. Kawakami, S. Koyanagi, T. Yamabe, and M. Shiro, *Chem. Lett.*, **1992**, 2321.
- 2 S. Kimura, H. Kurai, T. Mori, H. Mori, and S. Tanaka, *Bull. Chem. Soc. Jpn.*, **74**, 59 (2001).
- 3 S. Kimura, H. Kurai, and T. Mori, *Mol. Cryst. Liq. Cryst.*, in press.
- 4 M. Aragaki, S. Kimura, M. Katsuhara, H. Kurai, and T. Mori, *Bull. Chem. Soc. Jpn.*, **74**, 833 (2001).
- 5 T. Mori, H. Inokuchi, Y. Misaki, H. Nishikawa, T. Yamabe, H. Mori, and S. Tanaka, *Chem. Lett.*, **1993**, 733.
- 6 T. Mori, *Bull. Chem. Soc. Jpn.*, **71**, 2509 (1998).
- 7 S. Horiuchi, H. Yamochi, G. Saito, K. Sakaguchi, and M. Kusunoki, *J. Am. Chem. Soc.*, **118**, 8604 (1996).
- 8 T. Mori, H. Inokuchi, Y. Misaki, H. Nishikawa, T. Yamabe, H. Mori, and S. Tanaka, *Chem. Lett.*, **1993**, 2085.
- 9 Y. Misaki, H. Nishikawa, K. Kawakami, T. Yamabe, T. Mori, H. Inokuchi, H. Mori, and S. Tanaka, *Chem. Lett.*, **1993**, 2073.
- 10 M. Aragaki, T. Mori, Y. Misaki, K. Tanaka, and T. Yamabe, *Synth. Met.*, **102**, 1601 (1999).
- 11 T. Suzuki, H. Yamochi, G. Srdanov, K. Hinkelmann, and F. Wudl, *J. Am. Chem. Soc.*, **111**, 3108 (1989); A. M. Kini, T. Mori, U. Geiser, S. M. Budz, and J. M. Williams, *J. Chem. Soc., Chem. Commun.*, **1990**, 647.
- 12 N. Svenstrup, K. M. Rasmussen, T. K. Hansen, and J. Becher, *Synthesis*, **1994**, 809.
- 13 P. Wu, G. Saito, K. Imaeda, Z. Shi, T. Mori, T. Enoki, and H. Inokuchi, *Chem. Lett.*, **1986**, 441.
- 14 T. Mori, H. Mori, and S. Tanaka, *Bull. Chem. Soc. Jpn.*, **72**, 179 (1999).